Progress In Electromagnetics Research M, Vol. 71, 189–197, 2018

Broadband and Low-Profile Slot Antenna with AMC Surface for X/Ku Applications

Xue Yan Song*, Tian Ling Zhang, and Ze Hong Yan

Abstract—A low-profile and broadband slot antenna with artificial magnetic conductor (AMC) surface is designed for X and Ku communications. Loaded with evolved C-shaped branches, the proposed coplanar waveguide (CPW)-fed slot antenna, which consists of two radiating slots, exhibits wide impedance frequency band performance. The presented AMC, the unit cell of which is made up of two central hexagonal circles with six rectangle branches, operates in a wide in-phase reflection frequency band ranging from 6.0 to 13.94 GHz (79.64%) at the reference plane 4 mm above the AMC surface. An AMC surface composed of 8×10 AMC unit cells is located under the slot antenna with a distance of approximately 0.107λ (λ denotes the free-space wavelength at 8.0 GHz), which improves the radiation and impedance match properties of the broadband slot antenna while maintaining low profile. A prototype of the proposed slot antenna with AMC surface is fabricated and measured. Measured results show that the composite antenna achieves a wide impedance bandwidth from 7.64 to 14.58 GHz (62.47%). The measured peak gain is up to 10.26 dBi, and the maximum cross-polarization level is -17.5 dB for both E and H planes. Good agreements between the measured and simulated results validate good performance of the presented slot antenna within the desired frequency band.

1. INTRODUCTION

With the rapid development of modern wireless communication technologies, low-profile and broadband planar microstrip antennas have received considerable attention owing to their simple structure, good radiation efficiency and ease of fabrication and integration with active devices. Among them, slot antennas can provide greater bandwidth, more stable performance, and have better manufacturing tolerances [1–3]. However, slot antennas radiate bidirectionally, and a PEC ground plane has to be placed under slot antennas with a distance of a quarter wavelength to achieve good unidirectional radiation performance and high gain, which will bring in large antenna height.

To achieve low profile and enhanced radiation performance simultaneously, AMC [4] has been intensely proposed and widely utilized because of their in-phase reflection property recently. In the in-phase reflection frequency band, the phase values would not cause destructive interference between incident and reflected waves [5]. Therefore, an AMC surface can be served as the antenna ground plane to obtain low profile and improved radiation performances [6–8]. Researches on utilization of AMC surface as ground plane of planar slot antennas have been carried out in the past few years [9–12]. In [9], Joubert et al. propose a low-profile CPW-fed slot antenna with an AMC reflector, which exhibits a 5% impedance bandwidth, a height of $0.063\lambda_0$ and a maximum gain in excess of 10 dBi. A novel combination of CPW-fed double bow-tie slot antenna and AMC is presented in [10], which achieves a relative bandwidth of about 19.6%, extremely low profile and an enhanced gain. A reconfigurable folded slot antenna integrated with a polarization-dependent dual-band AMC surface is designed for a

Received 18 June 2018, Accepted 1 August 2018, Scheduled 10 August 2018

* Corresponding author: Xue Yan Song (xysong6597@126.com).

The authors are with the National Key Laboratory of Antennas and Microwave Technology, Xidian University, Xi'an, Shaanxi 710071, China.

wearable remote patient monitoring system in [11], which achieves improved radiation performance and a low distance of approximately $\lambda/20$ between the antenna and AMC surface. Reference [12] proposed a dual-band textile antenna loaded with an AMC plane, which achieves an extremely low profile and a relatively wide band covering 2.4 and 5 GHz bands for WLAN applications. By using AMC surface as the ground plane, the slot antennas discussed in [9–12] achieve low profile and enhanced gain performances. However, the bandwidths are less than 20%.

To obtain a wider band and low-profile planar antenna, a planar CPW-fed slot antenna is firstly designed in this paper, which exhibits a simulated relative bandwidth of 52.4%. Then, an adaptation of a broadband AMC surface is designed and etched beneath the slot antenna with a distance of approximately 0.107λ as the ground plane, as shown in Figure 1. Simulated results demonstrate that the combined antenna exhibits a 52.88% (8.04–13.82 GHz) impedance bandwidth and a maximum gain of 10.48 dBi.

2. THE PROPOSED ANTENNA DESIGN AND CONFIGURATION

2.1. The Proposed Slot Antenna Design

The geometry of the designed CPW-fed slot antenna with dimensions is shown in Figure 1, which is etched on the top side of an F4BM-2 dielectric substrate with a thickness of 0.5 mm, relative dielectric permittivity of 2.65 and loss tangent of 0.002. From Figure 1, the designed slot antenna consists of two radiating slots with evolved C-shaped branches, which is designed from the L-slot antenna depicted in Figure 2(a). When loaded with C-shaped slot branches, the L-slot antenna becomes the slot antenna2 in Figure 2(b), and the impedance characteristic is improved, as shown in Figure 3. That is because by adding C-shaped slot branches on the L-shaped slot antenna, the length of the surface current path around the slot is increased [1]. This effect can be modeled as an additional series inductance ΔL. Moreover, an additional capacitance ΔC as a gap capacitance between the middle arm of the L-shaped antenna and the two arms of the C-shaped slot introduces. Therefore, new resonances close to the

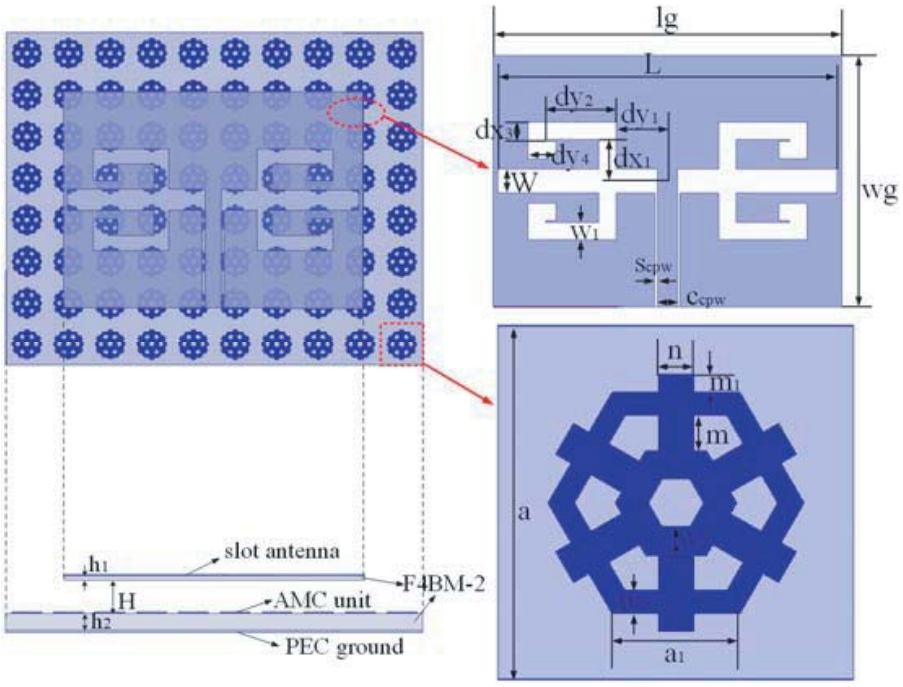

Figure 1. Top and side views of the composite antenna. Dimensions: $H = 4$, $h_1 = 0.5$, $h_2 = 2$, $wg = 26$, $lg = 36$, $L = 35$, $W = 2.5$, $Ccpw = 2$, $Scpw = 0.3$, $w_1 = 1.8$, $dx_1 = 4.3$, $dy_1 = 5.3$, $dy_2 = 7.3$, $dx_3 = 2$, $dy_4 = 2.9$, $a = 5$, $a_1 = 1.8$, $m_1 = 0.25$, $m = 0.5$, $n = 0.5$, $w_1 = 0.32$, $w_2 = 0.4$ (unit: mm).

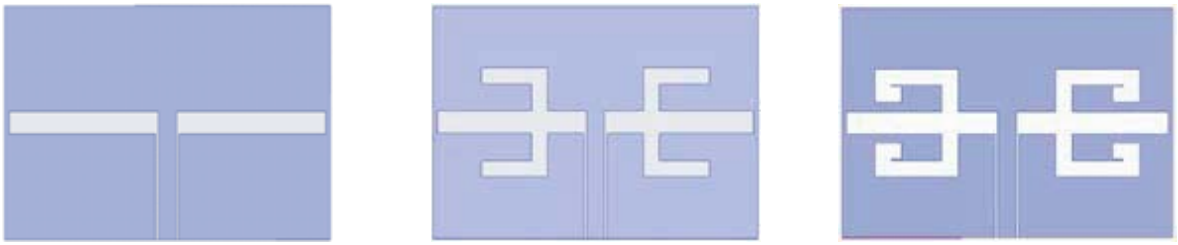

Figure 2. Geometry of the three types of slot antennas. (a) Slot antenna1, (b) slot antenna2 and (c) the proposed slot antenna.

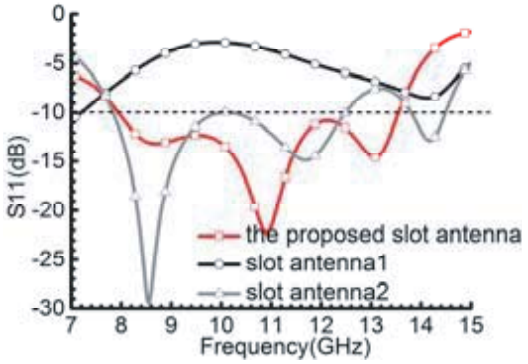

Figure 3. Simulated S_{11} of the three types of slot antennas.

main resonance of the L-shaped antenna are created [1]. Hence, multiple resonances are generated, which contributes to the broadband property. To further improve the impedance characteristic, two L-shaped branches are added on the ends of each C-shaped branch, which gives birth to the proposed slot antenna. From Figure 3, it can be seen that the S_{11} curve of the proposed slot antenna is lower than those of slot antenna1 and slot antenna2, and the operation band ranges from 8.0 to 13.68 GHz, which illuminates broadband performance.

2.2. AMC Surface Design

An AMC is made up of a frequency selective surface (FSS) printed on a grounded dielectric substrate. When the AMC structure is located under the incidence of a plane wave, it exhibits a reflection coefficient of +1 at a specified frequency [13]. It means that the phase of the reflected wave is 0° compared to that of the incident wave, which enables the AMC surface to produce constructive superposition of the incident and reflected waves [14]. The frequency band, in which the reflection phase ranges from −90° to +90°, is defined as the in-phase band of the AMC structure [4]. Therefore, using an AMC surface as ground plane, antennas can achieve low profile and enhanced radiation performance.

To improve the radiation property of the presented slot antenna, the AMC surface should exhibit an in-phase reflection frequency band covering its impedance frequency band (8.0–13.68 GHz) discussed above. Therefore, an AMC surface with the merit of wide in-phase reflection band is demanded. Since it has a first-mode resonant frequency two times that of other ring types with the exception of the square spiral element and its second resonance is approximately three times that of the fundamental one, the hexagonal ring has superior bandwidth characteristic [15]. Hence, the presented AMC unit cell is made up of two concentric hexagonal circles with six rectangle branches as depicted in Figure 1. It is realized on a 2-mm-thick grounded F4BM-2 substrate ($\varepsilon_r = 2.65$, $\tan\delta = 0.002$), without any ground via.

The reflection phase characteristics are simulated by using an ANSYS HFSS Floquet-port model, and Figure 4(a) shows the simulated model of the proposed AMC unit cell. What is depicted in

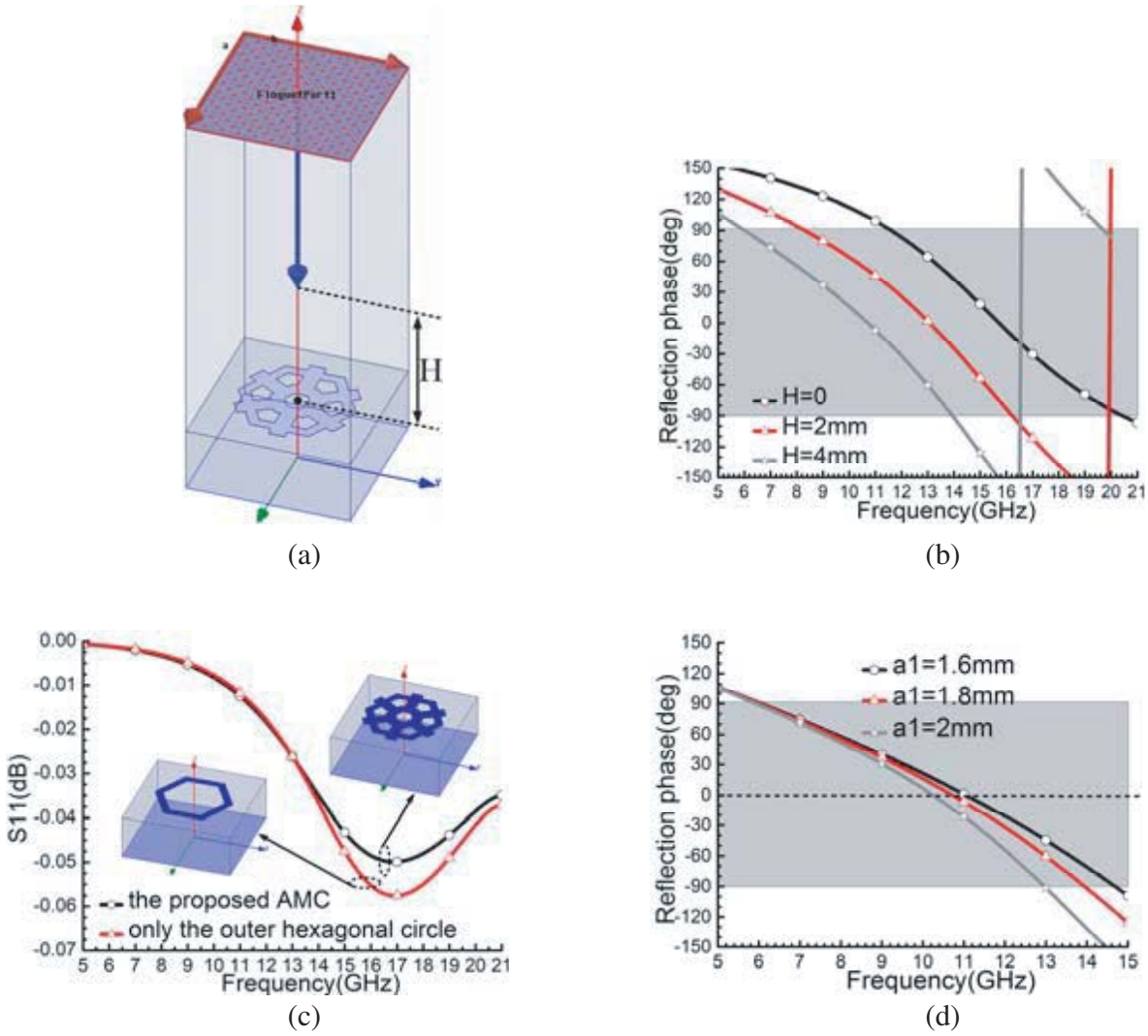

Figure 4. (a) The simulated model of the proposed AMC unit cell; (b) Simulated reflection phase of the proposed AMC at different reference plane H above the AMC; (c) Comparison of S_{11} between the proposed AMC unit cell and the outer hexagonal circle; (d) Simulated reflection phase of the proposed AMC with different $a1$ at the reference plane $H = 4\,\text{mm}$ above the AMC.

Figure 4(b) is the simulated reflection phase of the proposed AMC at different reference plane with a distance of H above the AMC surface. It can be obtained that the designed AMC offers an in-phase bandwidth of about 56% (11.6–20.45 GHz). However, there is an increase in reflection phase bandwidth and a decrease in the resonance frequency when the reference plane is moved away from the AMC surface. When the reference plane is at 4 mm above the AMC plane, the in-phase frequency band can reach to 79.64% (6.0–13.94 GHz) which can cover the operation band (8.0–13.68 GHz) of the slot antenna discussed above. Actually, the AMC unit cell made up of the only outer hexagonal circle can provide the required in-phase reflection frequency band. However, the reflection loss is a little high. To decrease the reflection loss and make more energy be reflected to normal direction, an inner hexagonal circle with six rectangle branches is added on the outer hexagonal circle. As can be seen in Figure 4(c), the reflection loss is decrease by using the proposed AMC unit cell. Of all the parameters, parameter $a1$ has the most significant effect on the in-phase frequency band of the designed AMC, which is demonstrated in Figure 4(d). Each AMC unit cell can be modeled as a distributed parallel LC network that has one or more resonant frequencies. The resonant frequency, near which the impedance is very high, is equal

to $1/(2\pi\sqrt{LC})$, while in-phase reflection relative bandwidth is proportional to $\sqrt{L/C}$ [4, 13, 16]. With the increase in parameter $a1$, the coupling capacitance C between two adjacent unit cells increases, thus decreasing both the resonant frequency and the in-phase frequency band, as depicted in Figure 4(d). Although the bandwidth is wider when $a1 = 1.6$ mm, the 0° reflection phase appears at 11.05 GHz. The effect of AMC surface on the gain of the designed slot antenna in low frequency band will be weakened. Hence, 1.8 mm is finally selected as the value of parameter $a1$.

Hence, it can be observed from Figure 4(d) that the 0° reflection phase occurs at 10.72 GHz, and the ultra-wide in-phase frequency band of the AMC structure ranges from 6.0 to 13.94 GHz (79.64%) when the reference plane is at 4 mm above the AMC plane, where the planar slot is located in the antenna design. The in-phase band covers the operation frequency band of the slot antenna previously discussed.

2.3. The Proposed Slot Antenna Loaded with AMC Surface

The geometry of the presented slot antenna with AMC surface is depicted in Figure 1. The size of the AMC surface also influences the behavior of the combined antenna, especially the front-back-ratio. A larger size brings in a higher front-back-ratio. Take an example of the radiation pattern at 10.5 GHz, the front-back-ratio of the combined antenna is higher than 20 dB when the AMC surface consists of 10×12 unit cells, as shown in Figure 5(a). When the AMC surface is made up of 6×8 unit cells, the front-back-ratio is about 12 dB, as shown in Figure 5(c). For compromise of high front-to-back ratios and small size, the AMC surface consists of 8×10 unit cells, with dimensions of $40 \times 50\,\text{mm}^2$. The bandwidth and the impedance matching property of the composite antenna are closely related with the distance between the slot antenna and the AMC surface, H. A decrease in H leads to good impedance matching and wide bandwidth, especially in high frequency band, as can be observed from Figure 6(a). That is because when H decreases, the in-phase frequency band of AMC surface moves to high frequency, as shown in Figure 6(b), and has better influence on the performance of the antenna in high frequency band. However, small distance will result in high cross polarization caused by the coupling between the slot antenna and the AMC surface. Therefore, $H = 4$ mm is finally chosen for low-profile, good impedance matching and low cross polarization purpose.

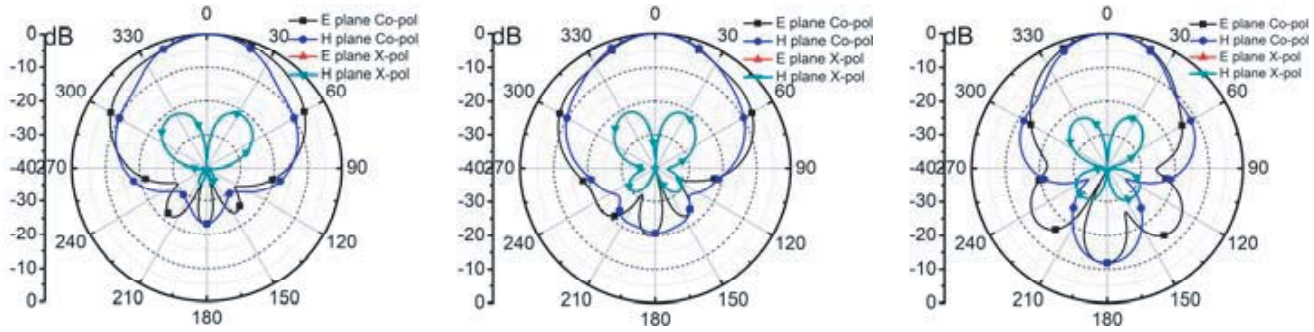

Figure 5. Radiation patterns of the proposed antenna at 10.5 GHz for different sizes of the AMC plane. (a) 10×12 unit cells, (b) 8×10 unit cells, and (c) 6×8 unit cells.

To further investigate the mechanism of the designed antenna, a detailed study on the slot antenna with and without AMC is conducted for comparison. Figure 7 plots the simulated reflection coefficients of the proposed slot antenna over the AMC surface. For comparison, the slot antenna without the ground plane is also simulated. It displays that the −10 dB bandwidths of the slot antenna with and without AMC surface are 8.0–13.68 GHz and 8.04–13.82 GHz, respectively. It can be observed that the impedance characteristic is improved when the slot antenna is mounted with the AMC surface. Figure 8 demonstrates the simulated gain of the slot antenna and the combined antenna, from which it can be summarized that the gain can be improved up to approximately 3 dB when the slot antenna is located on the AMC surface. Moreover, the maximum gain of the composite antenna can reach 10.48 dBi.

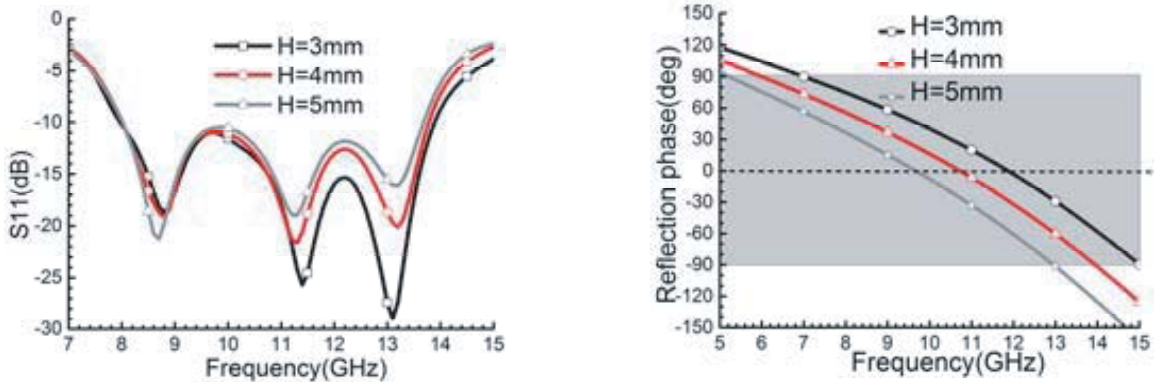

(a) (b)

Figure 6. (a) Simulated S_{11} of the combined antenna with different H; (b) Simulated reflection phase of the proposed AMC at the distance of different H.

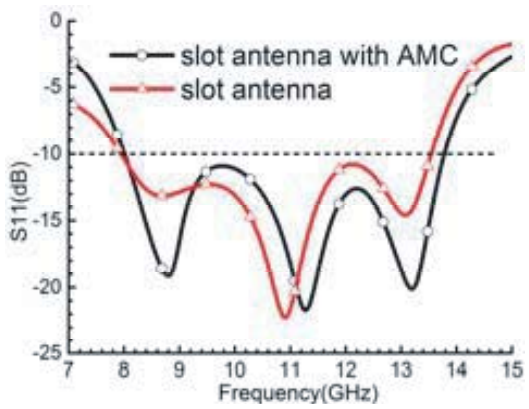

Figure 7. Simulated S_{11} of the slot antenna with and without AMC.

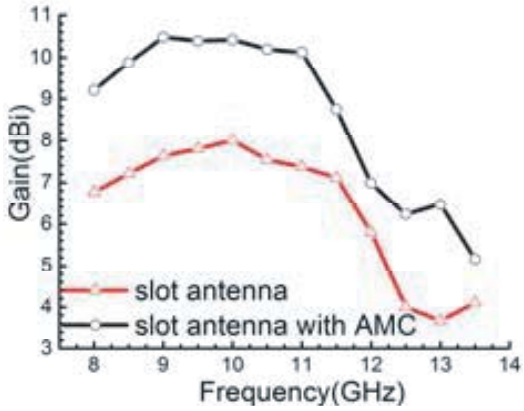

Figure 8. Simulated gain of the slot antenna with and without AMC.

Therefore, the broadband slot antenna loaded with AMC surface achieves improved gain property while maintaining low profile. It can also be noted that there is a decrease of gain in high frequency band. That is because the beam widths of the proposed slot antenna at high frequencies become wider than that at low frequencies.

3. EXPERIMENT AND SIMULATION RESULTS AND DISCUSSIONS

The prototype of the designed slot antenna over the AMC structure is finally fabricated as shown in Figure 9(a) and practically measured in the anechoic chamber as depicted in Figure 9(b). The designed antenna is placed as high as the transmitting horn antenna and at a distance of 1.5 m from the horn antenna to satisfy the far field requirement. The reflection coefficient of the prototype is measured using an Agilent E8363B vector network analyzer and compared with the simulated results in Figure 10. It can be noted that the combined antenna operates in the frequency band ranging from 7.64 GHz to 14.58 GHz (62.47%), while the simulated relative impedance bandwidth is 52.88% (8.04 GHz to 13.82 GHz). The discrepancies between the measured and simulated results are on account of the fabrication and measurement errors together with the effect of the SMA connector.

In addition, Figure 11 depicts the simulated and measured gains and radiation efficiency at different frequencies, which exhibits a measured maximum gain in excess of 10.26 dBi, a high antenna efficiency over 80% and a good agreement except for a little distinction due to the fabrication and measurement error and metal plating process in fabrication. The radiation patterns of the designed antenna are

(a) (b)

Figure 9. (a) Photograph of the proposed slot antenna and AMC; (b) Experiment environment in the anechoic chamber.

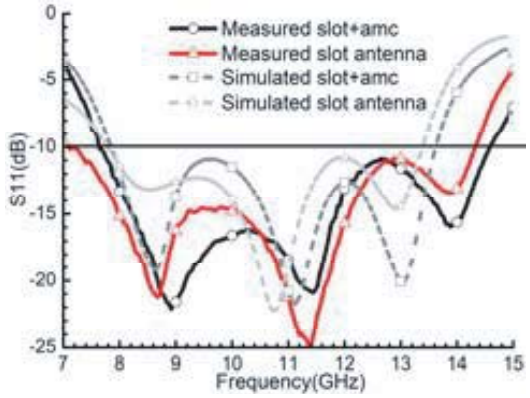

Figure 10. Measured and simulated S_{11} of the proposed antenna.

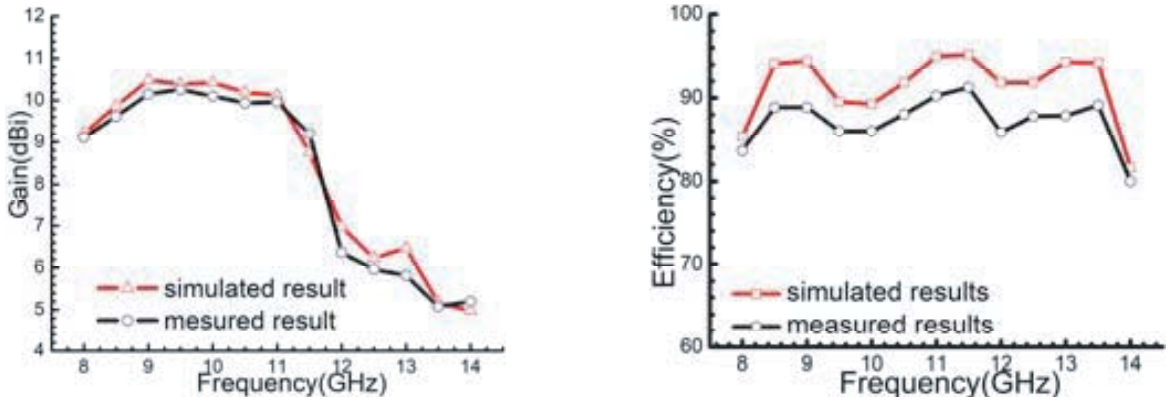

(a) (b)

Figure 11. Measured and simulated (a) gain and (b) radiation efficiency of the proposed combined antenna.

examined at 9, 10.5 and 12 GHz in two principle cut planes, which are compared with the simulated ones, as plotted in Figure 12. The results show that good consistency at the three operating frequencies exists in between the measured and simulated patterns. It can also be obtained from the measured results that the maximum cross-polarization level is -17.5 dB for both E and H planes and the front-to-back ratios at the three frequencies are higher than 18 dB.

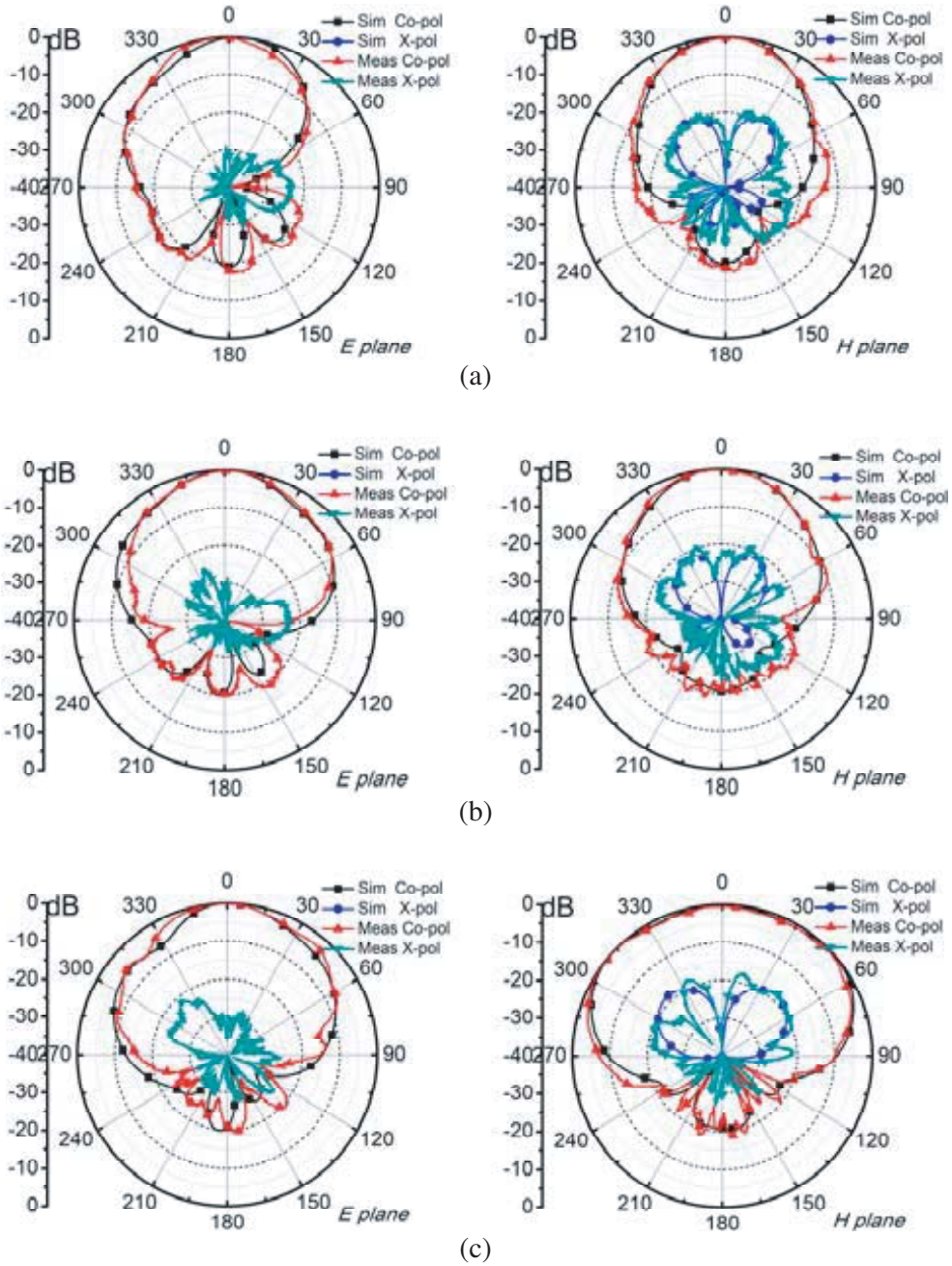

Figure 12. Measured and simulated radiation patterns of the proposed antenna at (a) 9 GHz, (b) 10.5 GHz and (c) 12 GHz.

4. CONCLUSION

In this paper, a broadband slot antenna loaded with evolved C-shaped branches is firstly designed. Then, an AMC surface composed of 8×10 unit cells, which has the merit of wide in-phase reflection band, is presented and mounted beneath the slot antenna with a small distance for gain enhancement and low profile. The measured results show that the composite antenna can operate from 7.64 GHz to 14.58 GHz (62.47%) and exhibit a maximum gain of up to 10.26 dBi, high front-to-back ratios and low cross-polarization level, which enable the proposed antenna to be utilized in X and Ku communications.

ACKNOWLEDGMENT

This work is supported by the National Natural Science Foundation of China (61401339) and the Fundamental Research Funds for the Central Universities (JB150229).

REFERENCES

1. Malekpoor, H. and S. Jam, "Improved radiation performance of low profile printed slot antenna using wideband planar AMC surface," *IEEE Trans. Antennas Propag.*, Vol. 64, No. 11, 4626–4638, 2016.
2. Mohamed-Hicho, N. M., E. Antonino-Daviu, M. Cabedo-Fabrés, J. P. Ciafardini, and M. Ferrando-Bataller, "On the interaction of characteristic modes in slot antennas etched on finite ground planes," *2016 European Conf. on Antennas Propag. (EuCAP)*, 1–5, 2016.
3. Ghaffarian, M. S., G. Moradi, and P. Mousavi, "Wide-band circularly polarized slot antenna by using novel feeding structure," *2017 European Conf. on Antennas Propag. (EuCAP)*, 2172–2175, 2017.
4. Sievenpiper, D., L. Zhang, R. F. J. Broas, N. G. Alexopolous, and E. Yablonovitch, "High-impedance electromagnetic surfaces with a forbidden frequency band," *IEEE Trans. Microw. Theory Tech.*, Vol. 47, No. 11, 2059–2074, 1999.
5. Feresidis, A. P., G. Goussetis, S. Wang, and J. C. Vardaxoglou, "Artificial magnetic conductor surfaces and their application to low-profile high-gain planar antennas," *IEEE Trans. Antennas Propag.*, Vol. 53, No. 1, 209–215, 2005.
6. Foroozesh, A. and L. Shafai, "Investigation into the application of artificial magnetic conductors to bandwidth broadening, gain enhancement and beam shaping of low profile and conventional monopole antennas," *IEEE Trans. Antennas Propag.*, Vol. 59, 4–20, 2011.
7. Vallecchi, A., J. R. Luis, F. Capolino, and F. D. Flaviis, "Low profile fully planar folded dipole antenna on a high impedance surface," *IEEE Trans. Antennas Propag.*, Vol. 60, No. 1, 51–62, 2012.
8. Song, X.-Y., C. Yang, T. Zhang, Z.-H. Yan, and R. Lian, "Broadband and gain enhanced bowtie antenna with AMC ground," *Progress In Electromagnetics Research Letters*, Vol. 61, 25–30, 2016.
9. Joubert, J., J. C. Vardaxoglou, W. G. Whittow, and J. W. Odendaal, "CPW-fed cavity-backed slot radiator loaded with an AMC reflector," *IEEE Trans. Antennas Propag.*, Vol. 60, No. 2, 735–742, 2012.
10. Hadarig, R. C., M. E. Cos Gomez, Y. Álvarez, and F. Las-Heras, "Novel bow-tie-AMC combination for 5.8-GHz RFID tags usable with metallic objects," *IEEE Antennas Wireless Propag. Lett.*, Vol. 9, 1217–1220, 2010.
11. Saeed, S. M., C. A. Balanis, C. R. Birtcher, A. C. Durgun, and H. N. Shaman, "Wearable flexible reconfigurable antenna integrated with artificial magnetic conductor," *IEEE Antennas Wireless Propag. Lett.*, Vol. 16, 2396–2399, 2017.
12. Yan, S., P. J. Soh, and G. A. E. Vandenbosch, "Low-profile dual-band textile antenna with artificial magnetic conductor plane," *IEEE Trans. Antennas Propag.*, Vol. 62, No. 12, 6487–6490, 2014.
13. Hadarig, R. C., M. E. Cos, and F. Las-Heras, "Novel miniaturized artificial magnetic conductor," *IEEE Antennas Wireless Propag. Lett.*, Vol. 12, 174–177, 2013.
14. Yang, W. C., H. Wang, W. Q. Che, Y. Huang, and J. Wang, "High-gain and low-loss millimeter-wave LTCC antenna array using artificial magnetic conductor structure," *IEEE Trans. Antennas Propag.*, Vol. 63, No. 1, 390–395, 2015.
15. Munk, B. A., *Frequency Selective Surfaces: Theory and Design*, Wiley, New York, NY, USA, 2000.
16. Cos, M. E., Y. Álvarez, and F. Las-Heras, "Novel broadband artificial magnetic conductor with hexagonal unit cell," *IEEE Antennas Wireless Propag. Lett.*, Vol. 10, 615–618, 2011.